

Investigation of Infrared Photo-Detection Through Subgap Density-of-States in a-InGaZnO Thin-Film Transistors

Heesung Lee, Junyeap Kim, Jaewon Kim, Seong Kwang Kim, Yongwoo Lee, Jae-Young Kim, Jun Tae Jang, Jaewon Park, Sung-Jin Choi, Dae Hwan Kim, and Dong Myong Kim

Abstract—Amorphous InGaZnO (a-IGZO) thin-film transistors (TFTs) are investigated for a possible application to infrared (IR) photodetector through subgap density-of-states over the forbidden bandgap. The origin of the sub-bandgap ($h\nu < E_g$) photo-response in a-IGZO TFTs is due to optically pumped electrons from the photo-responsive subgap states ($E_C - E_{ph} < E_t < E_F$). Among the sub-bandgap lights, we investigate the reproducible IR photo-response in a-IGZO TFTs as a photodetector without the persistent photoconductivity (PPC) effect. In this letter, we characterize the IR photo-response mechanism through various optical and electrical measurements on the wavelength, optical power, bias-modulated quasi-Fermi level, and photo-responsive states. This result is expected to provide independent and/or integrated IR detector with transparent substrate combined with a-IGZO TFTs.

Index Terms—Oxide semiconductor, IGZO, amorphous, infrared light, IR, photodetector, density-of-states, DOS, thin-film transistor, TFT.

I. INTRODUCTION

AMORPHOUS InGaZnO (a-IGZO) thin-film transistors (TFTs) have attracted much attention for various applications such as driving or switching devices in flexible and/or transparent displays as well as touch sensors and image sensors, due to their low-temperature deposition process, large-area uniformity, high field-effect mobility, high on/off ratio, and transparency to visible light [1]–[5]. In particular, transparent phototransistors that don't require any additional fabrication process are being actively studied. Because the a-IGZO has a wide bandgap ($E_g > 3$ eV), above-bandgap

light such as the ultraviolet (UV) light response is being studied [6]. Also, narrow bandgap materials such as silver nanoparticles, graphene dots, and quantum dots are used with a-IGZO to enhance the visible light response [7]–[9]. However, the infrared (IR) light reactivity in a-IGZO TFTs has yet to be reported.

Here, for the first time as far as we know, we report characterization of the IR photo-response mechanism through the subgap ($E_V < E < E_C$) density-of-states (DOS) over the bandgap of a-IGZO TFTs. We note that the energy distribution of the subgap DOS is the key parameter in the electrical characteristics [10], [16]. It is well known that the growing process and the resultant atomic composition of multicomponent metal-oxides determine the density and the energy distribution of subgap DOS [11]. We focused on the IR photo-detection by separation of electrons generated from the photo-responsive subgap states ($E_C - E_{ph} < E_t < E_F$) and ionized oxygen vacancies. This is also expected to be useful for reliability investigation in the negative gate bias illumination stress (NBIS) and positive gate bias illumination stress (PBIS). In order to characterize the photo-response mechanism under IR illumination, we adopt intensive optical power preventing devices from degradation for the distinct reaction. This result is expected to provide transparent photodetector and/or integrated sensor combined with a-IGZO TFTs in display systems.

II. MECHANISM OF INFRARED PHOTO-RESPONSE AND DEMONSTRATION BY ASSEMBLING VARIOUS OPTICAL AND ELECTRICAL MEASUREMENTS

The origin of the IR light response in a-IGZO TFTs is the optically pumped electrons from the photo-responsive subgap states ($E_C - E_{ph} < E_t < E_F$) as shown in Figs. 1(a) and (b). Under the IR light illumination in the a-IGZO layer, electrons filled at the subgap density-of-states (DOS) are pumped by photon energy. The number of only optically excited electrons per unit volume from photo-responsive states (N_{photo} [cm^{-3}]) is modeled to be

$$N_{photo} [\text{cm}^{-3}] \propto \left\{ \begin{array}{l} \int_{E_C - E_{ph}(\lambda)}^{E_F(V_{GS})} f(E) g(E) dE [\text{cm}^{-3}] \\ N_{inj,ph} = P_{opt} / (A \cdot h\nu) [\text{cm}^{-2}\text{s}^{-1}] \end{array} \right. \quad (1)$$

with $f(E)$ as the distribution function, $g(E)$ [$\text{eV}^{-1}\cdot\text{cm}^{-3}$] as the subgap DOS, E_F as the quasi-Fermi level, V_{GS} as the gate-source voltage, E_C as the conduction-band minimum, $E_{ph}(=h\nu)$ as the photon energy, λ [nm] as the wavelength, A as the illumination area and $N_{inj,ph}$ as the photon density

Manuscript received March 9, 2017; revised March 21, 2017; accepted March 21, 2017. Date of publication March 23, 2017; date of current version April 24, 2017. This work was supported by the National Research Foundation of Korea (NRF) grant funded by the Korean Government (MSIP) (2017R1A2B4007820 and 2016R1A5A 1012966), and in part by the Korea Foundation for the Advancement of Science and Creativity (KOFAC) grant funded by Ministry of Education (MOD). The review of this letter was arranged by Editor Shouu-Jinn Chang. (Heesung Lee and Junyeap Kim contributed equally to this work.) (Corresponding author: Dong Myong Kim.)

H. Lee, J. Kim, J. Kim, S. K. Kim, Y. Lee, J.-Y. Kim, J. T. Jang, S.-J. Choi, D. H. Kim, and D. M. Kim are with the School of Electrical Engineering, Kookmin University, Seoul 136-702, South Korea (e-mail: dmkim@kookmin.ac.kr).

J. Park is with the Department of Electrical and Electronic Engineering, South University of Science and Technology of China, Shenzhen 518055, China.

Color versions of one or more of the figures in this letter are available online at <http://ieeexplore.ieee.org>.

Digital Object Identifier 10.1109/LED.2017.2686844

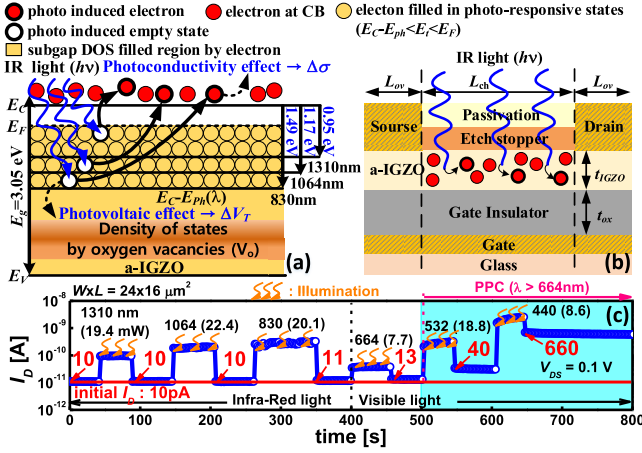


Fig. 1. (a) Energy band diagram of a-IGZO and the optically pumped electrons from the photo-responsive range ($E_C - E_{ph} < E_t < E_F$) for the photoconductive and photo-voltaic effect under IR light illumination. (b) Bottom gate a-IGZO TFT structure and generated electrons by IR light illumination. (c) Sub-bandgap photo-response as a function of the wavelength. Regardless of the photocurrent, only green ($\lambda = 532$ nm) and blue ($\lambda = 440$ nm) lights induce a persistent photoconductivity effect.

per second injector to the a-IGZO layer, P_{opt} [W] as the total optical power provided by the optical source which is regularly calibrated for accurate power output.

When sub-bandgap photons ($E_{ph} = h\nu < E_g$) are injected in a-IGZO TFTs, optically pumped electrons induce photoconductive effect and the empty subgap DOS charges cause the photovoltaic effect. We note that the lights having a wavelength shorter than $\lambda = 550$ nm, such as green (532 nm) and blue (440 nm), doubly ionize (V_O^{2+}) the oxygen vacancies (V_O) in the a-IGZO layer [12]. The transition from V_O to V_O^{2+} generates two electrons in the conduction band (CB). Because the ionized V_O can't be immediately recovered, ionization of V_O induces the persistent photoconductivity (PPC) effect [13]. As observed in Fig. 1(c), we note that only the current after illumination by $\lambda = 532$ nm is kept at 40 [pA] (increased from 13 [pA]) even though the currents under dark and under illumination are monitored the same for both $\lambda = 830$ nm and $\lambda = 532$ nm. It suggests that the PPC effect is only induced when the electrons are directly pumped from the energy level with V_O to CB by photons. Here, we consider only reproducible IR photo-detection which does not disturb the electrical parameters such as mobility, threshold voltage, and subthreshold swing for a possible application of the transparent a-IGZO TFT to IR photodetector either as an independent sensor and/or integrated transparent detectors combined with a-IGZO TFT driver circuits in high performance display systems.

When a-IGZO layer is illuminated by the IR light as shown in Fig. 1(a), photons excite electrons filled in the subgap DOS over the photo-responsive energy range ($E_C - E_{ph} < E_t < E_F$) while suppressing the direct band-to-band electron-hole-pair (ehp) generation from the valence band. These photo-generated electrons from the photo-responsive DOS levels contribute to the photo-conductivity change and threshold voltage change by the photo-voltaic effect caused by the charge state change in the subgap DOS in a-IGZO TFTs. The photo-induced increase in the conductivity can be described

as

$$\sigma \left[\Omega^{-1} \cdot \text{cm}^{-1} \right] = \sigma_o + \Delta\sigma = q (n_o + N_{photo}) \mu_{n,eff} \quad (2)$$

with σ_o as the conductivity in the dark, $\Delta\sigma$ as the photo-conductivity, $\mu_{n,eff}$ [$\text{cm}^2 \cdot \text{V}^{-1} \cdot \text{s}^{-1}$] as the effective electron mobility, and n_o [cm^{-3}] as the electron concentration in the dark. The photo-induced decrease (ΔV_T) in the threshold voltage (V_T) can be described as

$$V_T [\text{V}] = V_{T_o} - \Delta V_T; \quad \Delta V_T \equiv \frac{q N_{photo, sheet}}{C_{ox}} \quad (3)$$

with V_{T_o} as the dark state threshold voltage and $C_{ox} (= \epsilon_{ox}/t_{ox})$ [F/cm^2] as the oxide capacitance per unit area. $N_{photo, sheet}$ [cm^{-2}] as the photo-generated sheet carrier density from the photo-responsive energy range can be modeled as

$$N_{photo, sheet} \left[\text{cm}^{-2} \right] = \int_0^{t_{IGZO}} N_{photo} dx \quad (4)$$

with x [cm] as the distance in the active thickness direction and t_{IGZO} [nm] as the active layer thickness. The sub-threshold drain current ($I_{D, SUB}$) of the a-IGZO TFT as an accumulation mode metal-insulator-semiconductor field effect transistor (MISFET) [14], [16] is modeled to be

$$I_{D, SUB} \cong I_{D_o} e^{(V_{GS} - (V_{T_o} - \Delta V_T)) / m V_{th}} [\text{A}] \quad (V_{DS} > 3V_{th})$$

$$I_{D_o} = \mu_{n,eff} C_{ox} \left(\frac{W}{L} \right) (m - 1) V_{th}^2 [\text{A}] \quad (5)$$

with $V_{th} (= kT/q)$ [V] as the thermal voltage, m as the substrate coupling factor, (W/L) as the gate width-to-length ratio, and V_{DS} as the drain voltage. We also note that the linear mode ($V_{DS} \ll V_{GS} - V_T$) drain current (I_D) [15] is modeled to be

$$I_D \approx \mu_{n,eff} C_{ox} \left(\frac{W}{L} \right) (V_{GS} - (V_{T_o} - \Delta V_T)) V_{DS} [\text{A}]. \quad (6)$$

III. EXPERIMENTAL RESULTS AND DISCUSSION

In the characterization of the photo-response mechanism for the IR light through the subgap DOS, we employed n-channel inverted staggered a-IGZO TFTs on a glass substrate. After deposition of the gated electrode (Mo) by RF sputtering, a gate insulator (SiO_x) was deposited by plasma enhanced chemical vapor deposition (PECVD). Then, a-IGZO (In:Ga:Zn = 1:1:1) thin-film was deposited by DC sputtering in a gas mixture of $\text{Ar}/\text{O}_2 = 35/48$ at room temperature (RT). The source/drain (Mo) layer and the etch stopper (SiO_2) was formed by DC sputtering and PECVD on the a-IGZO thin film, respectively. Finally, a passivating layer (SiO_x) was formed by PECVD and a-IGZO thin-film was annealed at $T = 523\text{K}$ for 1 hour.

The gate width, length, and overlap length are designed to be $W/L/L_{ov} = 10/10/6 \mu\text{m}$ SiO_x with $t_{ox} = 200$ nm as the gate dielectric and $t_{IGZO} = 30$ nm for the a-IGZO active layer as shown in Fig. 1(b). As shown in Fig. 2 for the transfer characteristic ($I_D - V_{GS}$), we obtain $V_{T_o} = 0.1$ V and subthreshold swing (SS) = 370 mV/dec. In the characterization, we used an Agilent 4156C parameter analyzer and IR laser diode (LD) with wavelengths of $\lambda = 830$ nm, 1064 nm, and 1310 nm to characterize the photo-detection mechanism

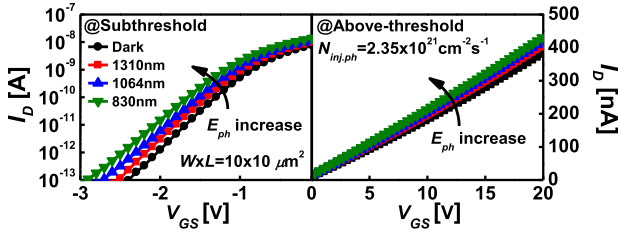


Fig. 2. Photo-responsive transfer characteristic (I_D - V_{GS}) of a-IGZO TFTs under IR light illumination with $\lambda = 830$ nm, 1064 nm, and 1310 nm in the subthreshold and above-threshold regions.

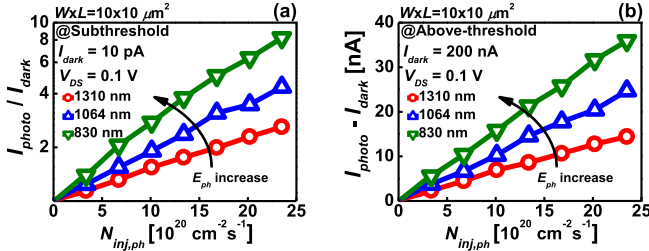


Fig. 3. (a) I_{photo}/I_{dark} (log scale) versus $N_{inj,ph}$ consistent with Eqs. (1), (3), and (5). (b) $I_{photo}-I_{dark}$ versus $N_{inj,ph}$ consistent with Eqs. (1), (3), and (6) as a function of the wavelength.

through the subgap DOS in a-IGZO TFTs. We guided photons through the optical fiber with a diameter $d = 50 \mu\text{m}$ to the a-IGZO photo-responsive region by the Cascade optical microprobe. In this work, the optical fiber end covers the entire area of the active a-IGZO layer in the device under test. Therefore, the optical power density is calculated to be $P_{opt}/[\pi(d/2)^2] (= N_{inj,ph} E_{ph})$ [W/cm²].

In order to investigate the IR light response through the subgap DOS in a-IGZO TFTs, we combined various optical and electrical characterization with P_{opt} [W] and the wavelength ($\lambda = 830$ nm, 1064 nm, and 1310 nm). For comparative characterization, we set the optical power $P_{opt} = 1 \sim 7$ mW to be $N_{inj,ph} = 3.36 \times 10^{20} \text{ cm}^{-2} \cdot \text{s}^{-1} \sim 23.5 \times 10^{20} \text{ cm}^{-2} \cdot \text{s}^{-1}$ for $\lambda = 1310$ nm.

As shown in Figs. 3(a) and (b), I_{photo}/I_{dark} is exponentially proportional to $N_{inj,ph}$ in the subthreshold region and $I_{photo}-I_{dark}$ is linearly proportional to $N_{inj,ph}$ in the linear mode operation in the above-threshold region. This means that ΔV_T is proportional to $N_{inj,ph}$ and consistent with Eqs. (1), (3), (5), and (6). Also, as shown in Fig. 1(a), the photo-responsive states ($E_C-E_{ph} < E_t < E_F$) increases and consequently the IR light reactivity increases on the basis of Eq. (1) for short wavelength photons.

We also investigated photo-responsive modulation of I_D for the variation of E_F controlled by the gate bias. In order to set a uniform distribution of E_F over the channel from the source to the drain, we set V_{DS} as small as 0.1 V. As shown in Fig. 4(b), by changing I_D from 100 nA to 300 nA, E_F is expected to be close to E_C . Consequently, the photo-responsive energy range ($E_C-E_{ph} < E_t < E_F$) goes to maximum and the IR light reactivity increases consistent with Eq. (1).

We investigated photo-response from the increased $g(E)$ by ionization of oxygen vacancies with short wave length illumination. As shown in Fig. 4(a), we illuminated photons with $\lambda = 440$ nm (blue) while maintaining P_{opt} at 8 mW for 3500 s. The saturated photocurrent in Fig. 4(a) indicates that

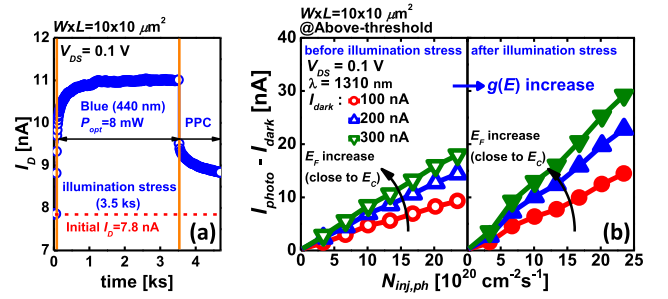


Fig. 4. (a) Blue-light illumination stress for increased $g(E)$ by ionization of oxygen vacancies. (b) $I_{photo}-I_{dark}$ versus $N_{inj,ph}$ consistent with Eq. (1) as a function of the quasi-Fermi level controlled by the gate bias and $g(E)$.

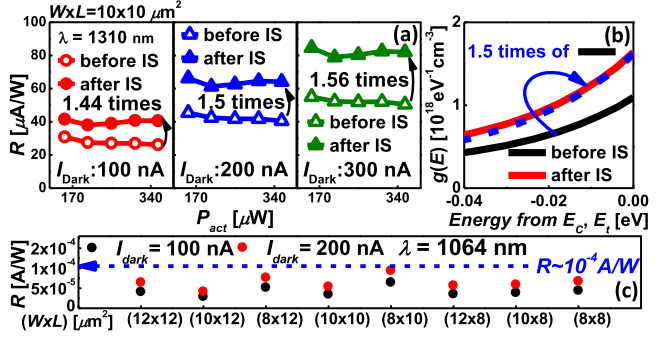


Fig. 5. (a) Infrared ($\lambda = 1310$ nm) photo-responsivity versus P_{act} . (b) The subgap DOS before and after illumination stress. (c) Photo-responsivity of the devices fabricated through the same process.

V_O 's are fully ionized ($V_O \rightarrow V_O^{2+} + 2e^-$) and the number of photo-responsive states are increased [12]. As shown in Fig. 4(b), 5(a) and 5(b), the increased photo-responsivity from increased $g(E)$ by illumination stress induces improved IR photo-responsivity consistent with Eq. (1). The photo-responsivity can be described as

$$R \text{ [A/W]} \equiv \frac{I_{photo} - I_{dark}}{P_{act}}, P_{act} \text{ [W]} = N_{inj,ph} W \cdot L \cdot E_{ph} \quad (7)$$

with P_{act} as the optical power injected to the active layer. As shown in Fig. 5(c), the IR responsivity of the device fabricated through the same process is observed to be $\sim 10^{-5}$ A/W. Through the electro-optical measurement as a function of $N_{inj,ph}$, E_C-E_{ph} , E_F , and $g(E)$, we concluded the origin of the IR photo-response to be the subgap DOS.

IV. CONCLUSION

We investigated infrared photo-responsivity of a-IGZO TFTs for a possible application to infrared (IR) photodetector through the photo-responsive ($E_C-E_{ph} < E < E_F$) subgap density-of-states (DOS) over the forbidden bandgap. We characterized the IR photo-responsive mechanism for the sub-bandgap photons ($E_{ph} < E_g$) with various measurements variations on the optical power (P_{opt}), wavelength (λ), quasi-Fermi level controlled by the gate bias, and the photo-responsive subgap states ($g(E)$) generated by ionization of oxygen vacancies with short wave length illumination. This result is expected to be useful for implementation of independent and/or integrated IR detector with transparent substrate combined with a-IGZO TFTs in high performance display systems.

REFERENCES

- [1] K. Nomura, H. Ohta, A. Takagi, T. Kamiya, M. Hirano, and H. Hosono, "Room-temperature fabrication of transparent flexible thin-film transistors using amorphous oxide semiconductors," *Nature*, vol. 432, no. 4016, pp. 488–492, Nov. 2004, doi: 10.1038/nature03090.
- [2] S. Shi, D. Wang, J. Yang, W. Zhou, Y. Li, T. Sun, and K. Nagayama, "A 9.55-inch flexible top-emission AMOLED with a-IGZO TFTs," in *SID Symp. Dig. Tech. Papers*, Jul. 2014, vol. 45, no. 1, pp. 330–333, doi: 10.1002/j.2168-0159.2014.tb0089.x
- [3] G. J. Lee, J. Kim, J.-H. Kim, S. M. Jeong, J. E. Jang, and J. Jeong, "High performance, transparent a-IGZO TFTs on a flexible thin glass substrate," *Semicond. Sci. Technol.*, vol. 29, no. 3, p. 035003, Jan. 2014, doi: 10.1088/0868-1242/29/3/035003.
- [4] S. Jeon, S. Park, I. Song, J.-H. Hur, J. Park, S. Kim, S. Kim, H. Yin, E. Lee, S. Ahn, H. Kim, C. Kim, and U.-I. Chung, "180 nm gate length amorphous InGaZnO thin film transistor for high density image sensor applications," in *IEDM Tech. Dig.*, Dec. 2010, pp. 504–507, doi: 10.1109/IEDM.2010.5703406.
- [5] T.-Y. Hsieh, T.-C. Chang, T.-C. Chen, Y.-C. Chen, and Y. T. Chen, "Application of in-cell touch sensor using photo-leakage current in dual gate a-InGaZnO thin-film transistors," *Appl. Phys. Lett.*, vol. 101, no. 21, p. 212104, Nov. 2012, doi: 10.1063/1.4767912.
- [6] C.-S. Chuang, T.-C. Fung, B. G. Mullins, K. Nomura, T. Kamiya, H.-P. D. Shieh, H. Hosono, and J. Kanicki, "P-13: Photosensitivity of amorphous IGZO TFTs for active-matrix flat-panel displays," in *SID Symp. Dig. Techn. Papers*, May 2008, vol. 39, no. 1, pp. 1215–1218, doi: 10.1889/1.3069354.
- [7] J. Yu, S. W. Shin, K.-H. Lee, J.-S. Park, and S. J. Kang, "Visible-light phototransistors based on InGaZnO and silver nanoparticles," *J. Vac. Sci. Technol. B, Microelectron. Process. Phenom.*, vol. 33, no. 6, p. 061211, Nov. 2015, doi: 10.1116/1.4936113.
- [8] S. W. Shin, K. H. Lee, J. S. Park, and S. J. Kang, "Highly transparent, visible-light photodetector based on oxide semiconductors and quantum dots," *ACS Appl. Mater. Interfaces*, vol. 7, no. 35, pp. 19666–19671, Sep. 2015, doi: 10.1021/acsami.5b04683.
- [9] Z. Pei, H. C. Lai, J. Y. Wang, W. H. Chiang, and C. H. Chen, "High-responsivity and high-sensitivity graphene dots/a-IGZO thin-film phototransistor," *IEEE Electron Device Lett.*, vol. 36, no. 1, pp. 44–46, Jan. 2015.
- [10] M. Dai, K. Khan, S. Zhang, K. Jiang, X. Zhang, W. Wang, L. Liang, H. Cao, P. Wang, P. Wang, L. Miao, H. Qin, J. Jinag, L. Xue, and J. Chu, "A direct method to extract transient sub-gap density of state (DOS) based on dual gate pulse spectroscopy," *Sci. Rep.*, vol. 6, p. 24096, Jun. 2016, doi: 10.1038/srep24096.
- [11] E. Fortunato, P. Barquinha, and R. Martins, "Oxide semiconductor thin-film transistors: A review of recent advances," *Adv. Mater.*, vol. 24, no. 22, pp. 2945–2986, Jun. 2012, doi: 10.1002/adma.201103228.
- [12] J. H. Kim, U. K. Kim, Y. J. Chung, and C. S. Hwang, "Correlation of the change in transfer characteristics with the interfacial trap densities of amorphous In-Ga-Zn-O thin film transistors under light illumination," *Appl. Phys. Lett.*, vol. 98, no. 23, p. 232102, Jun. 2011, doi: 10.1063/1.3597299.
- [13] S. Jeon, S.-E. Ahn, I. Song, C. J. Kim, U.-I. Chung, E. Lee, I. Yoo, A. Nathan, S. Lee, K. Ghaffarzadeh, J. Robertson, and K. Kim, "Gated three-terminal device architecture to eliminate persistent photoconductivity in oxide semiconductor photosensor arrays," *Nature Mater.*, vol. 11, no. 4, pp. 301–305, Apr. 2012.
- [14] M. Bae, D. Yun, Y. Kim, D. Kong, H. K. Jeong, W. Kim, J. Kim, I. Hur, D. H. Kim, and D. M. Kim, "Differential ideality factor technique for extraction of subgap density of states in amorphous InGaZnO thin-film transistors," *IEEE Electron Device Lett.*, vol. 33, no. 3, pp. 399–401, Mar. 2012, doi: 10.1109/LED.2011.2182602.
- [15] I. Hur, H. Bae, W. Kim, J. Kim, H. K. Jeong, C. Jo, S. Jun, J. Lee, Y. H. Kim, D. H. Kim, and D. M. Kim, "Characterization of intrinsic field-effect mobility in TFTs by de-embedding the effect of parasitic source and drain resistances," *IEEE Electron Device Lett.*, vol. 34, no. 2, pp. 250–252, Feb. 2013.
- [16] H. Lee, J. Kim, S. Choi, S. K. Kim, J. Kim, J. Park, S.-J. Choi, D. H. Kim, and D. M. Kim, "Band-bending effect in the characterization of Subgap density-of-states in amorphous TFTs through fully electrical techniques," *IEEE Electron Device Lett.*, vol. 38, no. 2, pp. 199–202, Feb. 2017, doi: 10.1109/LED.2016.2636301.